



## Analytical treatment for synchronizing chaos through unidirectional coupling and implementation of logic gates

P R VENKATESH<sup>1,\*</sup>, A VENKATESAN<sup>1</sup> and M LAKSHMANAN<sup>2</sup>

<sup>1</sup>PG & Research Department of Physics, Nehru Memorial College (Autonomous), Puthanampatti, Tiruchirapalli 621 007, India

<sup>2</sup>Department of Physics, Centre for Nonlinear Dynamics, Bharathidasan University, Tiruchirapalli 620 024, India

\*Corresponding author. E-mail: venkatesh.sprv@gmail.com; av.phys@gmail.com; lakshman@cnd.bdu.ac.in

MS received 26 December 2014; revised 17 June 2015; accepted 21 August 2015

DOI: 10.1007/s12043-016-1199-5; ePublication: 8 April 2016

**Abstract.** The idea of synchronization can be explicitly demonstrated by both numerical and analytical means on a nonlinear electronic circuit. Also, we introduce a scheme to obtain various logic gate structures, using synchronization of chaotic systems. By a small change in the response parameter of unidirectionally coupled nonlinear systems, one is able to construct various logic behaviours by both numerical and analytical methods.

**Keywords.** Chaos; chaos synchronization.

**PACS Nos** 05.45.–a; 05.45.Pq; 05.45.Gg

### 1. Introduction

Driving a nonlinear system with a periodic signal is a common feature in nonlinear dynamics. However, the idea of using a chaotic signal to drive a nonlinear system and to maintain synchronization in phase and amplitude of the driving and the driven systems is rather new. The idea of synchronizing two identical chaotic systems starting from different initial conditions was first introduced by Fujisaka and Yamada [1–3] and Pecora and Carroll (PC) [4–7]. It consists of linking the trajectory of one system to the same values in the other so that they remain in step with each other forever after some transient time.

Nowadays, chaos synchronization is an active research topic in nonlinear science. Control theory [8], telecommunication [9–12], encoding message [13–16], laser dynamics [17,18], electronic circuits [19,20], chemical and biological systems [21,22] and secure communications [12] are some situations where chaos synchronization has been extensively studied.

In recent times, various methods of synchronization have been proposed and implemented, namely complete synchronization (CS) [1,4,23], generalized synchronization

(GS) [24–29], phase synchronization (PS) [30–34], lag synchronization (LS) [35–37] and anticipating synchronization (AS) [38]. Of various synchronization techniques, unidirectional coupling is one of the simplest and easiest one. The unidirectional coupling technique involves sending a system variable from the original system (sender or transmitter) to drive the replica (receiver); sometimes, the replica subsystem and the original chaotic one can lock in their states and evolve together chaotically in synchrony.

As the success of chaos synchronization depends strongly on the estimation of the coupling parameter  $\epsilon$ , it is of considerable interest and importance to find how minimum is the coupling parameter  $\epsilon$ . This minimum value of coupling parameter for synchronization is called critical value  $\epsilon_c$ . In the present work, we analytically estimate the critical value of the coupling parameter for chaotically synchronized piecewise nonlinear systems and the critical value is confirmed by numerical Runge–Kutta fourth (RK IV) order method. In this paper, the aim of chaos synchronization is to design and implement the dynamic logic gates which will help ‘chaos computing’. The idea of chaos computing [39–41] can be explicitly demonstrated with both analytical solutions and the numerical method for unidirectionally coupled identical piecewise nonlinear systems.

## 2. Two unidirectionally coupled identical Murali–Lakshmanan–Chua circuits

To look at the foregoing ideas in a concrete model, we consider a simple unidirectionally coupled nonlinear electronic circuit, namely, two identical Murali–Lakshmanan–Chua (MLC) [13,42–44] coupled systems for analysis as shown in figure 1.

By applying Kirchoff’s law, the dynamical equations can be represented as that of the drive (left in the circuit) and the response (right in the circuit) systems as follows:

Drive system:

$$\begin{aligned}
 C \frac{dv}{dt} &= i_L - g(v), \\
 L \frac{di_L}{dt} &= -Ri_L - R_S i_L - v + f(t),
 \end{aligned}
 \tag{1}$$

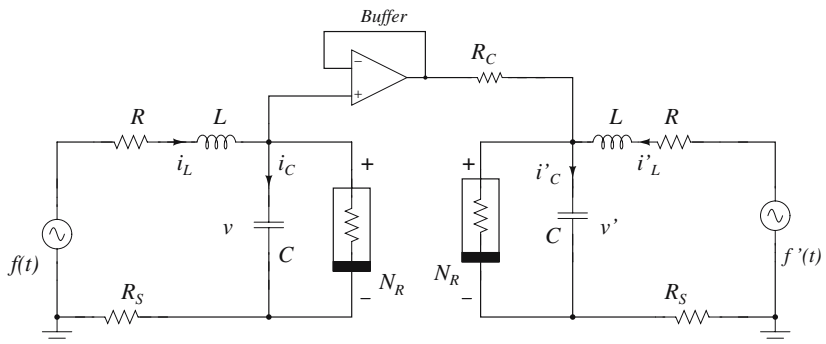


**Figure 1.** Two unidirectionally coupled MLC circuits.

where

$$g(v) = \begin{cases} m_0 v + (m_0 - m_1) B_p, & v < -B_p \\ m_1 v, & -B_p \leq v \leq B_p \\ m_0 v + (m_1 - m_0) B_p, & v > B_p \end{cases}$$

Response system:

$$\begin{aligned} C \frac{dv'}{dt} &= i'_L - g(v') - \epsilon(v - v'), \\ L \frac{di'_L}{dt} &= -Ri'_L - R_s i'_L - v' + f'(t), \end{aligned} \quad (2)$$

where

$$g(v') = \begin{cases} m_0 v' + (m_0 - m_1) B_p, & v' < -B_p \\ m_1 v', & -B_p \leq v' \leq B_p \\ m_0 v' + (m_1 - m_0) B_p, & v' > B_p \end{cases}$$

where  $v$  and  $i_L$  are respectively the voltage across the capacitor  $C$  and current through the inductor  $L$  in the drive system ( $v'$  and  $i'_L$  in the response system) and  $\epsilon = R/R_c$  is the coupling parameter. Here  $g(v)$  and  $g(v')$  represent the piecewise linear characteristic function of Chua's diode in the drive and the response system respectively. Also the values of the slopes and break point voltage of the Chua's diode are fixed as  $m_1 = -0.7$  ms,  $m_0 = -0.41$  ms and  $B_p = 1$  V. Further,  $f(t) = f_d \sin \Omega t$  and  $f'(t) = f_r \sin \Omega t$  are the external forces in the drive and the response systems.

For analytical and numerical confirmation, we rescale eqs (1) and (2) by redefining  $v = x B_p$ ,  $v' = x' B_p$ ,  $i_L = y G B_p$ ,  $i'_L = y' G B_p$ ,  $G = 1/R$ ,  $\omega = \Omega C/G$ ,  $t = \tau C/G$  and then change  $\tau$  as  $t$ . The set of normalized equations obtained after rescaling are as follows:

Drive system:

$$\begin{aligned} \dot{x} &= y - h(x), \\ \dot{y} &= -\beta(1 + v)y - \beta x + F_d \sin \omega t, \end{aligned} \quad (3)$$

where

$$h(x) = \begin{cases} bx + (a - b), & x > 1 \\ ax, & |x| \leq 1 \\ bx - (a - b), & x < -1 \end{cases} .$$

Response system:

$$\begin{aligned} \dot{x}' &= y' - h(x') - \epsilon(x - x'), \\ \dot{y}' &= -\beta(1 + v)y' - \beta x' + F_r \sin \omega t, \end{aligned} \quad (4)$$

where

$$h(x') = \begin{cases} bx' + (a - b), & x' > 1 \\ ax', & |x'| \leq 1 \\ bx' - (a - b), & x' < -1 \end{cases} .$$

and  $\beta = C/LG^2$ ,  $\nu = GR_s$ ,  $F_d = f_d\beta/B_p$ ,  $F_r = f_r\beta/B_p$ ,  $a = G_a/G$ ,  $b = G_b/G$ ,  $G_a = -0.76$  ms,  $G_b = -0.41$  ms and the parameters are fixed in the chaotic region.

The parameters are fixed at  $a = -1.02$ ,  $b = -0.55$ ,  $\nu = 0.015$ ,  $\beta = 1.0$ ,  $F_d = F_r = F = 0.4$  and  $\omega_1 = \omega_2 = \omega = 0.72$ . When  $\epsilon = 0$ , the two chaotic systems become uncoupled and desynchronized. When  $\epsilon$  increases from zero, the systems become coupled and then synchronized at a particular value called critical coupling parameter  $\epsilon_c$ .

### 3. Analytical solutions for the two coupled identical MLC circuits

Now the drive system (3) can be explicitly integrated in terms of elementary functions in each of the three regions  $D_0$ ,  $D_+$  and  $D_-$  ( $|x| \leq 1$ ,  $x > 1$  and  $x < -1$ ) and matched across the boundaries to obtain the full solution as shown below.

It is found that in each one of the regions  $D_0$ ,  $D_+$  and  $D_-$ , driving system (3) can be represented as a single second-order inhomogeneous differential equation for the variable  $y(t)$ ,

$$\ddot{y} + (\beta + \beta\nu + \mu)\dot{y} + (\beta + \mu\beta\nu + \beta\mu)y = \Delta + \mu F_d \sin \omega t + \omega F_d \cos \omega t, \quad (5)$$

where

$$\begin{aligned} \mu = a, \quad \Delta = 0 \text{ in region } D_0, \\ \mu = b, \quad \Delta = \pm\beta(a - b) \text{ in region } D_{\pm}. \end{aligned}$$

The general solution of the drive system (3) can be written as

$$y(t) = C_{0,\pm}^1 \exp(\alpha_1 t) + C_{0,\pm}^2 \exp(\alpha_2 t) + E_1 + E_2 \sin \omega t + E_3 \cos \omega t, \quad (6)$$

where  $C_{0,\pm}^1$  and  $C_{0,\pm}^2$  are integration constants in the appropriate regions  $D_0$ ,  $D_{\pm}$  and

$$\begin{aligned} A &= \beta + \beta\nu + \mu, \\ B &= \beta + \mu\beta\nu + \beta\mu. \\ \alpha_{1,2} &= (-A \pm \sqrt{A^2 - 4B})/2, \\ E_1 &= 0 \text{ in region } D_0, \\ E_1 &= \Delta/B \text{ in region } D_{\pm}, \\ E_2 &= \frac{[F_d\omega^2(A - \mu) + \mu F_d B]}{[A^2\omega^2 + (B - \omega^2)^2]}, \\ E_3 &= \frac{F_d\omega[B - \omega^2 - \mu A]}{[A^2\omega^2 + (B - \omega^2)^2]}. \end{aligned}$$

Knowing  $y(t)$ ,  $x(t)$  can be obtained from eq. (3) as

$$x(t) = \frac{1}{\beta}[-\dot{y} - \beta y(1 + \nu) + F_d \sin \omega t],$$

and so

$$\begin{aligned} x(t) = \frac{1}{\beta} \left[ -C_{0,\pm}^1(\alpha_1 + \sigma) \exp(\alpha_1 t) - C_{0,\pm}^2(\alpha_2 + \sigma) \exp(\alpha_2 t) \right. \\ \left. + (E_2\omega + E_3\sigma) \cos \omega t + (F_d - E_2\sigma + E_3\omega) \sin \omega t - E_1\sigma \right], \quad (7) \end{aligned}$$

where  $\sigma = \beta(1 + \nu)$ . While substituting the value of  $x(t)$  in the response system (4), we can get nine regions, namely  $D_{00}$ ,  $D_{0+}$ ,  $D_{0-}$ ,  $D_{+0}$ ,  $D_{++}$ ,  $D_{+-}$ ,  $D_{-0}$ ,  $D_{-+}$  and  $D_{--}$  ( $|x| \leq 1$  and  $|x'| \leq 1$ ,  $|x| \leq 1$  and  $x' > 1$ ,  $|x| \leq 1$  and  $x' < -1$ ,  $x > 1$  and  $|x'| \leq 1$ ,  $x > 1$  and  $x' > 1$ ,  $x > 1$  and  $x' < -1$ ,  $x < -1$  and  $|x'| \leq 1$ ,  $x < -1$  and  $x' > 1$  and  $x < -1$  and  $x' < -1$ ).

It is observed that in each one of the nine regions, the response system (4) can be represented as a single second-order inhomogeneous differential equation with the variable  $y'(t)$  as follows:

$$\begin{aligned} & \ddot{y}' + (\sigma + \mu' - \epsilon)\dot{y}' + (\beta + \sigma(\mu' - \epsilon))y' \\ & = (F_r(\mu' - \epsilon) + \epsilon F_d + \omega E'_1 - \sigma E'_2) \sin \omega t \\ & \quad + (F_r\omega - \omega E'_2 - \sigma E'_1) \cos \omega t \\ & \quad - E'_3\delta_1 \exp(\alpha_1 t) - E'_4\delta_2 \exp(\alpha_2 t) - E'_0, \end{aligned} \tag{8}$$

where,

$$E'_1 = \epsilon E_3, \quad E'_2 = \epsilon E_2,$$

with

$$\mu = \mu' = a, \quad E'_0 = 0, \quad \delta_1 = \delta_2 = 1, \quad E'_3 = \epsilon C_0^1[\sigma + \alpha_1],$$

$$E'_4 = \epsilon C_0^2[\sigma + \alpha_2]$$

in region  $D_{00}$ ,

$$\mu = a, \quad \mu' = b, \quad E'_0 = \epsilon\beta^2(a - b)(1 + \nu)/B,$$

$$\delta_1 = E'_3 \sin \alpha_2 t - E'_4 \cos \alpha_2 t, \quad \delta_2 = 0,$$

$$E'_3 = \epsilon[C_0^1\alpha_2 - C_0^2(\alpha_1 + \sigma)], \quad E'_4 = \epsilon[C_0^1(\alpha_1 + \sigma) + C_0^2\alpha_2]$$

in region  $D_{0+}$ ,

$$\mu = a, \quad \mu' = b, \quad E'_0 = \epsilon\beta^2(b - a)(1 + \nu)/B,$$

$$\delta_1 = E'_3 \sin \alpha_2 t - E'_4 \cos \alpha_2 t, \quad \delta_2 = 0,$$

$$E'_3 = \epsilon[C_0^1\alpha_2 - C_0^2(\alpha_1 + \sigma)], \quad E'_4 = \epsilon[C_0^1(\alpha_1 + \sigma) + C_0^2\alpha_2]$$

in region  $D_{0-}$ ,

$$\mu = b, \quad \mu' = a, \quad E'_0 = -\beta(a - b), \quad \delta_1 = \delta_2 = 1,$$

$$E'_3 = \epsilon C_+^1[\sigma + \alpha_1], \quad E'_4 = \epsilon C_+^2[\sigma + \alpha_2]$$

in region  $D_{+0}$ ,

$$\mu = \mu' = b, \quad E'_0 = \epsilon\beta^2(a - b)(1 + \nu)/B - \beta(a - b),$$

$$\delta_1 = E'_3 \sin \alpha_2 t - E'_4 \cos \alpha_2 t, \quad \delta_2 = 0,$$

$$E'_3 = \epsilon[C_+^1\alpha_2 - C_+^2(\alpha_1 + \sigma)], \quad E'_4 = \epsilon[C_+^1(\alpha_1 + \sigma) + C_+^2\alpha_2]$$

in region  $D_{++}$ ,

$$\mu = \mu' = b, \quad E'_0 = \epsilon\beta^2(b - a)(1 + \nu)/B - \beta(a - b),$$

$$\delta_1 = E'_3 \sin \alpha_2 t - E'_4 \cos \alpha_2 t, \quad \delta_2 = 0,$$

$$E'_3 = \epsilon[C_+^1\alpha_2 - C_+^2(\alpha_1 + \sigma)], \quad E'_4 = \epsilon[C_+^1(\alpha_1 + \sigma) + C_+^2\alpha_2]$$

in region  $D_{+-}$ ,

$$\begin{aligned} \mu &= b, \quad \mu' = a, \quad E'_0 = -\beta(b - a), \\ \delta_1 &= \delta_2 = 1, \quad E'_3 = \epsilon C_-^1[\sigma + \alpha_1], \quad E'_4 = \epsilon C_-^2[\sigma + \alpha_2] \end{aligned}$$

in region  $D_{-0}$ ,

$$\begin{aligned} \mu &= \mu' = b, \quad E'_0 = \epsilon\beta^2(a - b)(1 + \nu)/B - \beta(b - a), \\ \delta_1 &= E'_3 \sin \alpha_2 t - E'_4 \cos \alpha_2 t, \quad \delta_2 = 0, \quad E'_3 = \epsilon[C_-^1 \alpha_2 - C_-^2(\alpha_1 + \sigma)], \\ E'_4 &= \epsilon[C_-^1(\alpha_1 + \sigma) + C_-^2 \alpha_2] \end{aligned}$$

in region  $D_{-+}$ ,

$$\begin{aligned} \mu &= \mu' = b, \quad E'_0 = \epsilon\beta^2(b - a)(1 + \nu)/B - \beta(b - a), \\ \delta_1 &= E'_3 \sin \alpha_2 t - E'_4 \cos \alpha_2 t, \quad \delta_2 = 0, \quad E'_3 = \epsilon[C_-^1 \alpha_2 - C_-^2(\alpha_1 + \sigma)], \\ E'_4 &= \epsilon[C_-^1(\alpha_1 + \sigma) + C_-^2 \alpha_2] \end{aligned}$$

in region  $D_{--}$ .

By analytically solving these coupled differential equations by integrating in terms of elementary functions in nine different regions, namely  $D_{00}$ ,  $D_{0+}$ ,  $D_{0-}$ ,  $D_{+0}$ ,  $D_{++}$ ,  $D_{+-}$ ,  $D_{-0}$ ,  $D_{-+}$  and  $D_{--}$ , the general solution of the response system (4) can be written as

$$\begin{aligned} y'(t) &= \exp(\alpha_3 t) [C_{0\pm,0\pm}^3 \cos \alpha_4 t + C_{0\pm,0\pm}^4 \sin \alpha_4 t] + E'_c \cos \omega t \\ &+ E'_s \sin \omega t - \frac{E'_3 \exp(\alpha_1 t)}{(\alpha_1^2 + A'\alpha_1 + B')} - \frac{E'_4 \exp(\alpha_2 t)}{(\alpha_2^2 + A'\alpha_2 + B')} \\ &+ E'_5 \delta_5 \exp(\alpha_1 t) - \frac{E'_0}{B'}, \end{aligned} \tag{9}$$

where  $C_{0\pm,0\pm}^3$  and  $C_{0\pm,0\pm}^4$  are integration constants in the appropriate regions and

$$\begin{aligned} A' &= \sigma + \mu' - \epsilon, \\ B' &= \beta + (\mu' - \epsilon)\sigma, \\ \alpha_{3,4} &= \frac{(-A' \pm \sqrt{A'^2 - 4B'})}{2}, \\ E'_c &= \frac{[F_r \omega(B' - \omega^2) - (\mu' - \epsilon)\omega A'] - [(B' - \omega^2)(E'_1 \sigma + E'_2 \omega) + A' \omega(\epsilon F_d + E'_1 \omega - E'_2 \sigma)]}{[(B' - \omega^2)^2 + A'^2 \omega^2]}, \\ E'_s &= \frac{[F_r(\mu' - \epsilon)(B' - \omega^2) + \omega^2 A'] + [(B' - \omega^2)(\epsilon F_d + E'_1 \omega - E'_2 \sigma) - A' \omega(E'_1 \sigma + E'_2 \omega)]}{[(B' - \omega^2)^2 + A'^2 \omega^2]}, \\ E'_5 &= \frac{[(\alpha_1^2 - \alpha_2^2 + \alpha_1 A' + B')(C_{0\pm,0\pm}^1 \sin \alpha_2 t - C_{0\pm,0\pm}^2 \cos \alpha_2 t) - (2\alpha_1 + A')\alpha_2(C_{0\pm,0\pm}^1 \cos \alpha_2 t - C_{0\pm,0\pm}^2 \sin \alpha_2 t)]}{[(\alpha_1^2 - \alpha_2^2 + \alpha_1 A' + B')^2 + (2\alpha_1 + A')^2 \alpha_2^2]}, \\ \delta_5 &= 0 \text{ in regions } D_{00}, D_{+0} \text{ and } D_{-0}, \\ \delta_5 &= 1 \text{ in regions } D_{0+}, D_{0-}, D_{++}, D_{+-}, D_{-+} \text{ and } D_{--}. \end{aligned}$$

Knowing  $y'(t)$ ,  $x'(t)$  can be obtained from eq. (4) as

$$\begin{aligned}
 x'(t) = & \frac{1}{\beta} \left[ \exp(\alpha_3 t) [C_{0\pm,0\pm}^3 (\alpha_4 \sin \alpha_4 t - \alpha_3 \cos \alpha_4 t - \beta \sigma \cos \alpha_4 t) \right. \\
 & - C_{0\pm,0\pm}^4 (\alpha_3 \sin \alpha_4 t + \alpha_4 \cos \alpha_4 t + \beta \sigma \sin \alpha_4 t)] + \cos \omega t (-\omega E'_s - \sigma \beta E'_c) \\
 & + \sin \omega t (F_r + \omega E'_c - \sigma \beta E'_s) + \frac{E'_3 \exp(\alpha_1 t)}{(\alpha_1^2 + A' \alpha_1 + B')} [\alpha_1 + \beta \sigma] \\
 & \left. + \frac{E'_4 \exp(\alpha_2 t)}{(\alpha_2^2 + A' \alpha_2 + B')} [\alpha_2 + \beta \sigma] - E'_5 \delta_5 \exp(\alpha_1 t) [\alpha_1 + \beta \sigma] + \frac{E'_0}{B'} \right]. \quad (10)
 \end{aligned}$$

Thus, keeping  $F_d = F_r = F = 0.4$ ,  $\omega = 0.72$  and if we start with an initial condition in the  $D_{00}$  region, the corresponding arbitrary constants, namely  $C_0^1, C_0^2, C_0^3, C_0^4$ , can be found out. Then  $x(t)$  and  $x'(t)$  evolve using eqs (7) and (10) and the newly evolved values can be used to find the arbitrary constants of the solution for the new region of interest. This procedure can be continued upto  $t = T_1$ . The above procedure can be repeated for various values of the coupling parameter. From the obtained analytical solutions for the drive system from eqs (7) and (6) and for the response system from eq. (10) one can plot  $x$  vs.  $y$  and  $x$  vs.  $x'$  for various  $\epsilon$  values, namely  $\epsilon = 0.02, 0.06$  and  $0.2$  respectively as shown in figures 2a–2f. Also figure 2g explains how the synchronization error varies with  $\epsilon$  for the coupled MLC system. It has been found that for  $\epsilon_c = 0.053$  the coupled system becomes chaotically synchronized which is in good agreement with that of the numerically predicted values from figure 3g, i.e.,  $\epsilon_c = 0.06$  obtained by applying Runge–Kutta fourth-order method to the drive (3) and the response (4) systems. The dynamics of the drive and the response systems for various  $\epsilon$  values using numerical method is illustrated in figures 3a–3g.

#### 4. Implementation of logic gates using chaos synchronization

Computers, calculators and other digital devices are being magical and logical in their operations. The basic building block of any digital circuit is a logic gate. The basic logic gates are AND, OR and NOT. But the fundamental logic gate NOR can be used to build all the other gates. Further, XOR and AND gates can be used to perform the most fundamental bit-by-bit arithmetic addition operation. Other types of mathematical operations, namely subtraction (addition of the complement numbers), multiplication (repeated addition) and division (repeated subtraction) can also be easily performed using combined XOR and AND gates.

A system is capable of universal general purpose computing if it can emulate the basic logic operations NOR (universal gate), AND and XOR (building block of arithmetic operation). Note that the four sets of distinct possible inputs (two inputs) for NOR, XOR and AND gates (0, 0), (0, 1), (1, 0) or (1, 1) reduce to three conditions namely (0, 0), (0, 1) or (1, 0), and (1, 1). The input sets (0, 1) and (1, 0) are symmetric in their outputs for NOR (outputs 0), XOR (outputs 1) and AND (outputs 0) gates.

The computing element or logic gate is composed of unidirectionally coupled non-linear systems, namely unidirectionally coupled MLC systems (drive and response) represented by eqs (3) and (4), where  $a = -1.02$ ,  $b = -0.55$ ,  $\nu = 0.015$ ,  $\beta = 1.0$ ,  $\omega_1 = \omega_2 = \omega = 0.72$  and  $\epsilon = 1$ .

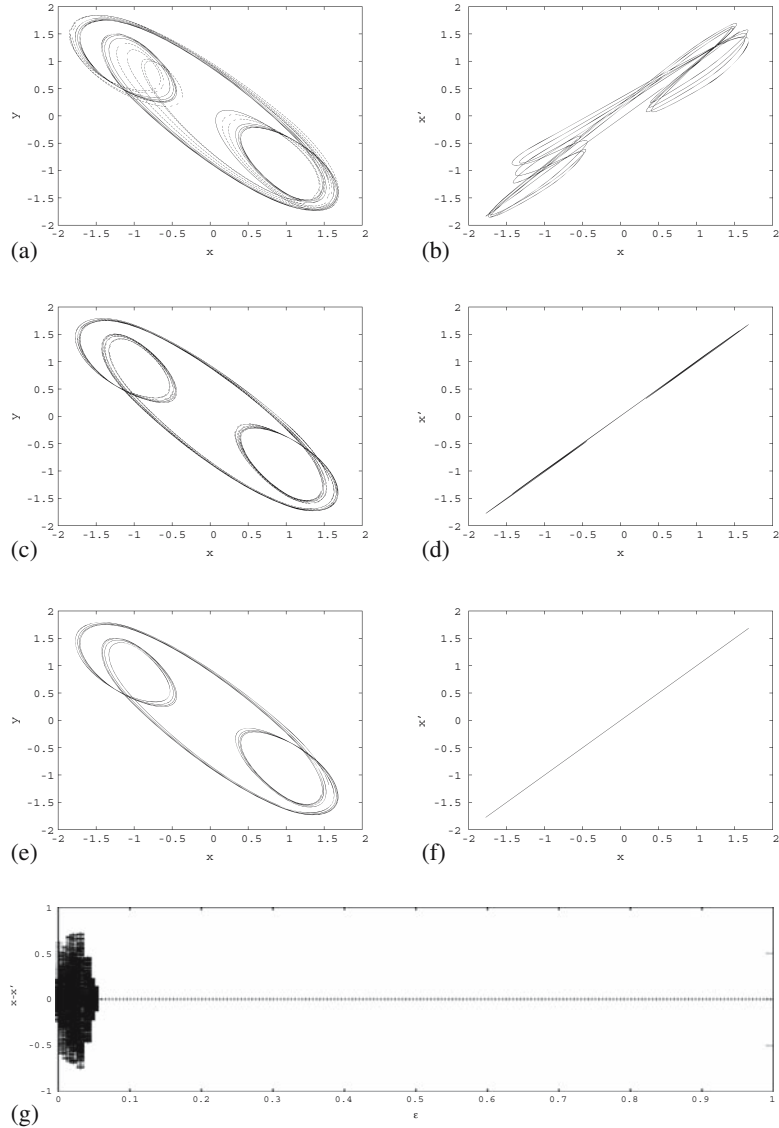


**Figure 2.** Using analytical solution (fixing  $F_d = F_r = F = 0.4$ ,  $\omega = 0.72$ ): (a) and (b) Unsynchronized output between the two unidirectionally coupled chaotic MLC circuits for  $\epsilon = 0.02$ . (c) and (d) Synchronized output between the two unidirectionally coupled chaotic MLC circuits for  $\epsilon = 0.053$ . (e) and (f) Perfectly synchronized output between the two unidirectionally coupled chaotic MLC circuits for  $\epsilon = 0.2$ . (g) Difference in trajectories between the drive and the response systems for various  $\epsilon$  values. In (a), (c) and (e) solid line represents the drive system and dotted line represents the response system.



*Implementation of logic gates through chaos synchronization*

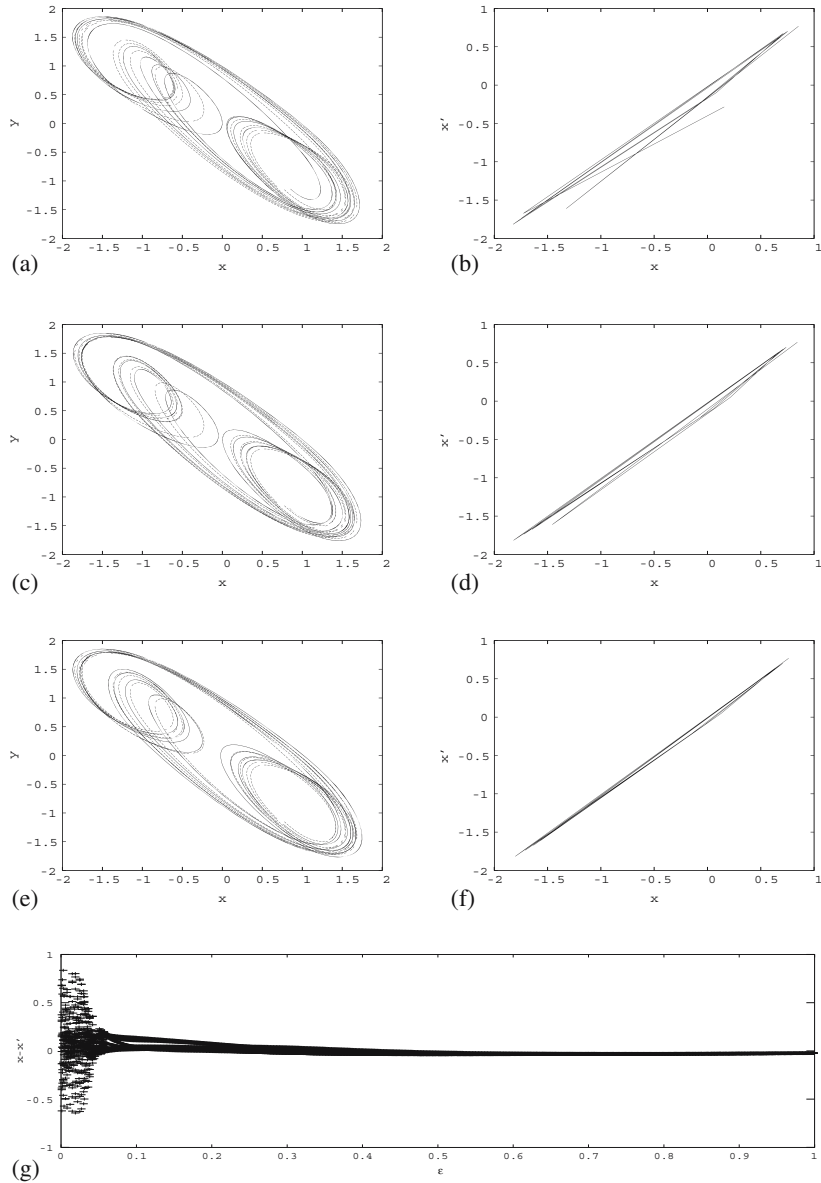


**Figure 3.** Using numerical RK fourth-order method (fixing  $F_d = F_r = F = 0.4$ ,  $\omega = 0.72$ ): (a) and (b) Unsynchronized output between the two unidirectionally coupled chaotic MLC circuits for  $\epsilon = 0.02$ . (c) and (d) Synchronized output between the two unidirectionally coupled chaotic MLC circuits for  $\epsilon = 0.06$ . (e) and (f) Perfectly synchronized output between the two unidirectionally coupled chaotic MLC circuits for  $\epsilon = 0.2$ . (g) Difference in trajectories between the drive and the response systems for various  $\epsilon$  values. In (a), (c) and (e) solid line represents the drive system and dotted line represents the response system.

The parameter of the drive system  $F_d$  is determined by the inputs and the parameter of the response system  $F_r$  acts as a logic gate controller. The synchronization error between the two systems comprising the computing element gives the logic output.

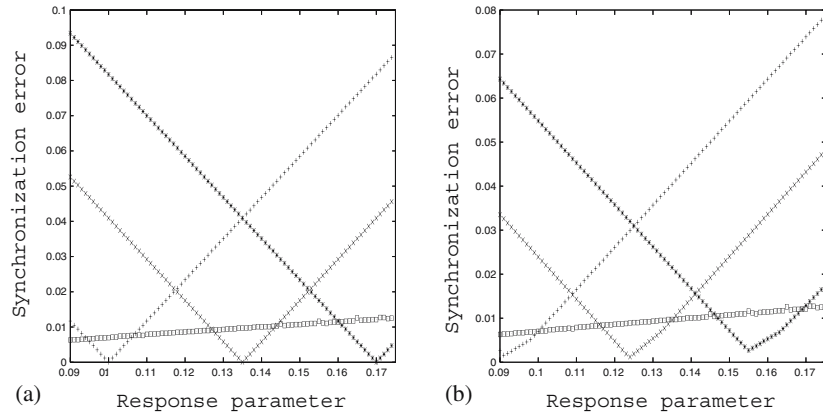
The input set  $(I_1, I_2)$  determines the drive parameter  $F_d$ , such that input set  $(0, 0)$  corresponds to  $F_{1d} = 0.1$ ,  $(0, 1)$  or  $(1, 0)$  corresponds to  $F_{2d} = 0.135$ , and  $(1, 1)$  corresponds to  $F_{3d} = 0.17$ , where  $F_{1d}$ ,  $F_{2d}$ ,  $F_{3d}$  are the three separate drive parameters in the chaotic region.

The logic gate controller identifies the type of logic operation which can be determined by the response parameter  $F_r$ , such that if  $F_r$  is set close to  $F_{1d}$ , one obtains NOR;  $F_r \approx F_{2d}$  for XOR and  $F_r \approx F_{3d}$  for AND.

The logic gate output is simply the synchronization error between the drive and the response systems: that is a large error in output is 0 and a small error in output is 1.

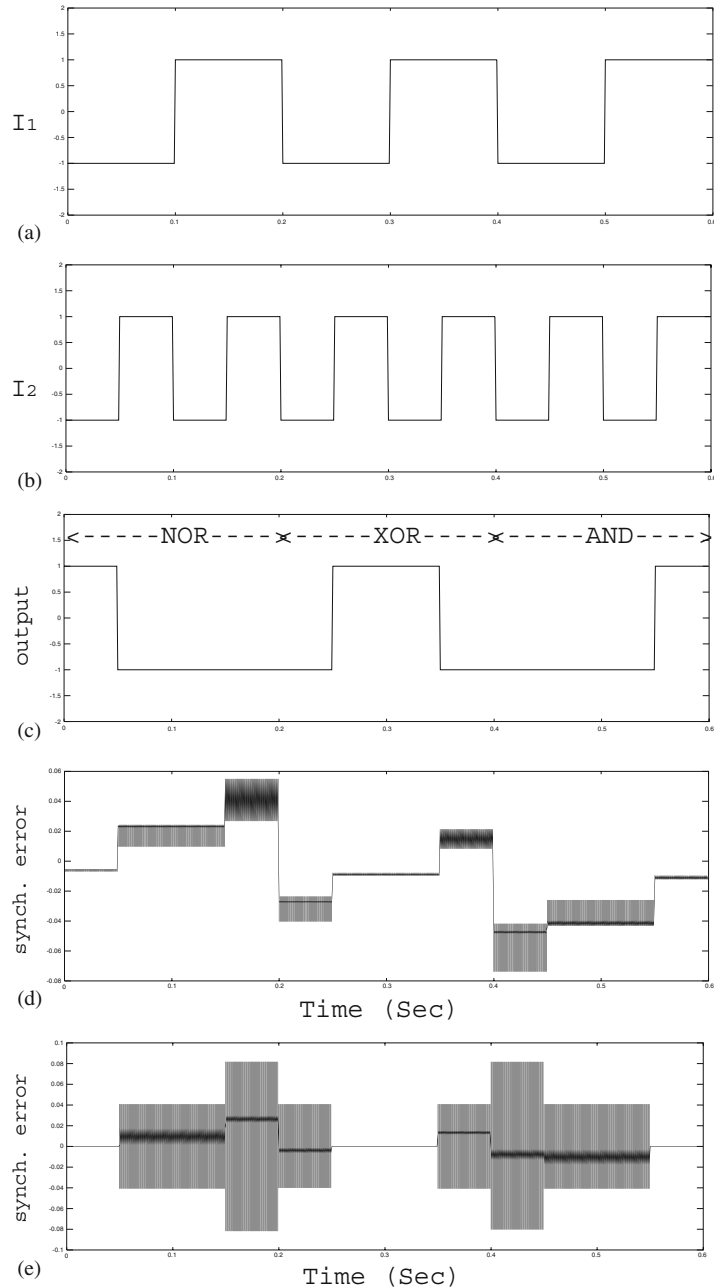
Numerical and analytical investigation of this system with respect to different sets of the drive and the response parameters ( $F_d$  and  $F_r$ ) yields the synchronization error displayed in figure 4. It is clear that by setting different response parameters  $F_r$  and appropriate synchronization errors  $x - x'$ , different logic gates can be obtained. In brief, we can take the output as 1, if the maximum of the absolute value of synchronization error is below 0.013, and the output as 0, if the absolute value of synchronization error is above 0.013. From figure 4, it is observed that the logic control parameter or response parameter for different logical operations are  $F_{rNOR} = 0.1$ ,  $F_{rXOR} = 0.135$  and  $F_{rAND} = 0.17$ .

Figure 5 shows the timing pulses of the dynamic NOR, XOR and AND gates. By adopting the fourth-order Runge–Kutta method to integrate eqs (3) and (4) in the computer simulation, the output (synchronization error) of the various logic gates (NOR, XOR and AND) can be obtained as shown in figure 5d. The numerical results agree completely with the results obtained by the analytical solutions (see figure 5e) from eqs (7) and (10).



**Figure 4.** Synchronization error envelope (maximum synchronization error) for the drive parameters:  $F_1 = 0.1$  corresponds to input set  $(I_1 = 0, I_2 = 0)$  (plus symbol);  $F_1 = 0.135$  corresponds to input set  $(I_1 = 0, I_2 = 1)/(I_1 = 1, I_2 = 0)$  (cross symbol);  $F_1 = 0.17$  corresponds to input set  $(I_1 = 1, I_2 = 1)$  (asterisk symbol). The horizontal line shows the maximum synchronization error obtained (numerical method) by keeping  $F_d = F_r$  and has an overall maximum value of 0.013 using (a) analytical solutions and (b) using numerical RK fourth-order method.

*Implementation of logic gates through chaos synchronization*



**Figure 5.** From top to bottom: (a) and (b) show a stream of input signals  $I_1$  and  $I_2$ , determining the input sets  $(I_1, I_2)$  say  $(0, 0)$ ,  $(0, 1)$ ,  $(1, 0)$ ,  $(1, 1)$  and repeated every 0.2 s in that order. (c) represents the dynamic logic response:  $[0 : 0.2 \text{ s}]$  is the NOR response,  $[0.2 : 0.4 \text{ s}]$  is the XOR response, and  $[0.4 : 0.6 \text{ s}]$  is the AND response. (d) represents the synchronization error obtained by numerical RK fourth-order method. (e) represents the synchronization error obtained by analytical solutions.

## 5. Conclusions

To sum up, the behaviour of the drive and the response systems are analytically found to be identical and hence the trajectories traced out by them are also identical for  $\epsilon_c = 0.053$  as in figures 2c and 2d and the synchronization seems to be perfect for  $\epsilon > 0.053$  as in figures 2e and 2f. For  $\epsilon < 0.053$ , the coupled system seems to be unsynchronized as in figures 2a and 2b. These analytical results are verified with the numerical method. Apart from that, we have also demonstrated the idea of implementation of logic gate structures which is one of the significance of synchronizations of nonlinear systems. In particular, we have shown the direct and flexible implementation of the basic logic gates NOR, XOR and AND, using a single drive–response system and the results have been verified by both numerical and analytical solutions. Such a scheme of implementation of basic logic gates for digital circuits may serve as ingredients of a general purpose device more flexible than statically wired hardware.

## Acknowledgements

The work of P R Venkatesh has been supported by Indian Academy of Sciences through its Summer Research Fellowship Programme (2008).

## References

- [1] H Fujisaka and T Yamada, *Prog. Theor. Phys.* **69**, 32 (1983)
- [2] H Fujisaka and T Yamada, *Prog. Theor. Phys.* **70**, 1240 (1983)
- [3] H Fujisaka and T Yamada, *Prog. Theor. Phys.* **72**, 885 (1984)
- [4] L M Pecora and T L Carroll, *Phys. Rev. Lett.* **64**, 821 (1990)
- [5] T L Carroll and L M Pecora, *Nonlinear dynamics in circuits* (World Scientific, Singapore, 1995)
- [6] T L Carroll and L M Pecora, *Physica D* **67**, 126 (1993)
- [7] T L Carroll, *Am. J. Phys.* **63**, 377 (1995)
- [8] K Pyragas, *Phys. Lett. A* **170**, 421 (1993)
- [9] K M Cuomo and A V Oppenheim, *Phys. Rev. Lett.* **71**, 65 (1993)
- [10] C W Wu and L O Chua, *Int. J. Bifurcation Chaos Appl. Sci. Eng.* **4**, 979 (1994)
- [11] R Brown, N F Rulkov and E R Tracy, *Phys. Rev. E* **49**, 3784 (1994)
- [12] L Kocarev and U Parlitz, *Phys. Rev. Lett.* **74**, 5028 (1995)
- [13] K Murali and M Lakshmanan, *Phys. Rev. E* **48**, R1624 (1993)
- [14] S Hayes, C Grebogi and W Ott, *Phys. Rev. Lett.* **70**, 3031 (1993)
- [15] U Parlitz and S Ergezinger, *Phys. Lett. A* **188**, 146 (1994)
- [16] U Parlitz, L Kocarev, T Stojanovski and H Preckel, *Phys. Rev. E* **53**, 4351 (1996)
- [17] L Fabiny, P Colet and R Roy, *Phys. Rev. A* **47**, 4287 (1993)
- [18] R Roy and K S Thornburg Jr, *Phys. Rev. Lett.* **72**, 2009 (1994)
- [19] V S Anisichenko *et al*, *Int. J. Bifurcation Chaos Appl. Sci. Eng.* **2**, 633 (1992)
- [20] J F Heagy, T L Carroll and L M Pecora, *Phys. Rev. A* **50**, 1874 (1994)
- [21] L Schreiber and M Marek, *Phys. D* **50**, 258 (1982)
- [22] S K Han, C Kurrer and K Kuramoto, *Phys. Rev. Lett.* **75**, 3190 (1995)
- [23] A S Landsman and I B Schwartz, *Phys. Rev. E* **75**, 026201 (2007)
- [24] N F Rulkov *et al*, *Phys. Rev. E* **51**, 980 (1995)
- [25] H D I Abarbanel *et al*, *Phys. Rev. E* **53**, 4528 (1996)

- [26] L M Pecora and U Parlitz, *Phys. Rev. Lett.* **76**, 1816 (1996)
- [27] K Pyragas, *Phys. Rev. E* **54**, R4508 (1996)
- [28] E M Shahverdiev and K A Shore, *Phys. Rev. E* **71**, 016201 (2005)
- [29] Z Zheng and G Hu, *Phys. Rev. E* **62**, 7882 (2000)
- [30] M G Rosenblum, A S Pikovsky and J Kurths, *Phys. Rev. Lett.* **76**, 1804 (1996)
- [31] G V Osipov, A S Pikovsky, M G Rosenblum and J Kurths, *Phys. Rev. E* **55**, 2353 (1997)
- [32] E Rosa, E Ott and M H Hess, *Phys. Rev. Lett.* **80**, 1642 (1998)
- [33] M A Zaks, E Park, M G Rosenblum and J Kurths, *Phys. Rev. Lett.* **82**, 4228 (1999)
- [34] D V Senthil Kumar, M Lakshmanan and J Kurths, *Phys. Rev. E* **74**, R035205 (2006)
- [35] M G Rosenblum, A S Pikovsky and J Kurths, *Phys. Rev. Lett.* **78**, 4193 (1997)
- [36] S Taherion and Y C Lai, *Phys. Rev. E* **59**, R6247 (1999)
- [37] M Chen and J Kurths, *Phys. Rev. E* **76**, 036212 (2007)
- [38] H U Voss, *Phys. Rev. E* **61**, 5115 (2000)
- [39] Sudeshna Sinha and William L Ditto, *Phys. Rev. E* **60**, 1063 (1999)
- [40] Toshinori Munakata, Sudeshna Sinha and William L Ditto, *IEEE Trans. Circuit and Systems I* **49**, 1629 (2002)
- [41] K Murali and Sudeshna Sinha, *Phys. Rev. E* **75**, R025201 (2007)
- [42] K Murali, M Lakshmanan and L O Chua, *IEEE Trans. Circuit and Systems I* **41**, 462 (1994)
- [43] M Lakshmanan and S Rajasekar, *Nonlinear dynamics: integrability, chaos and patterns* (Springer-Verlag, New York, 2003)
- [44] M Lakshmanan and K Murali, *Chaos in nonlinear dynamics: Controlling and synchronization* (World Scientific, Singapore, 1996)